Electronic Supplementary Information (ESI) for:

Ambipolar Charge Transport of TIPS-Pentacene Single-Crystals Grown from Non-Polar Solvents

Guobiao Xue,[a] Congcheng Fan,[a] Jiake Wu,[a] Shuang Liu,[a] Yujing Liu,[a] Hongzheng Chen,[a] Huolin L. Xin[b] and Hanying Li*[a]

[a]MOE Key Laboratory of Macromolecular Synthesis and Functionalization, State Key Laboratory of Silicon Materials, Department of Polymer Science and Engineering, Zhejiang University, Hangzhou 310027, P. R. China. E-mail: hanying_li@zju.edu.cn

[b]Center for Functional Nanomaterials, Brookhaven National Laboratory, Upton, NY 11973

Experimental section

TIPS-pentacene (Sigma-Aldrich) crystals were grown in ambient condition using the DPC method[1] onto the divinyltetramethyldisiloxane-bis(benzocyclobutene) (BCB)-covered highly doped silicon substrates (1 cm^2) with 300nm SiO_2.[2] BCB[3] (Dow Chemicals) thin-layers were spin-coated from a mesitylene (Fluka) solution (V_{BCB}:$V_{mesitylene}$ = 1:30) and, subsequently, thermally crosslinked on a hotplate in a N_2 glovebox. A TIPS-pentacene solution (10 μL, 0.4 mg/mL) in a specific solvent was dropped onto a silicon substrate (1 cm^2) with a smaller piece of silicon wafer (0.4 × 0.4 cm^2, pinner) to pin the solution droplet. The solvents used were hexane (TCI, HPLC), heptane (TCI, HPLC), cyclohexane (TCI, HPLC), CH_2Cl_2 (Aladdin, HPLC), $CHCl_3$ (Labor, HPLC) and THF (Aladdin, HPLC), respectively. The silicon substrate was placed on a Teflon slide inside a Petri-dish (35 mm × 10 mm) sealed with parafilm, allowing the solvent to slowly evaporate on a hotplate of 25 ± 1 ºC. Solution dried within forty minutes and aligned crystals formed. As a control experiment, the crystals were grown from mixed solvents of hexane and CH_2Cl_2 in different volume ratios ($V_{CH_2Cl_2}$: V_{hexane} = 1:1, 4:1, 8:1, respectively). The morphology of the crystals were characterized by optical microscopy (OM, Nikon LV100 POL) and Atomic force microscopy (AFM, Veeco 3D). Crystal thickness and width were measured by AFM from 10 ribbons. The crystalline structures were examined by selected-area electron diffraction (SAED, JEOL 1400). OFETs were constructed in a top contact, bottom-gate configuration by depositing electrodes (70 nm Au as both of the source and drain electrodes) using shadow masks (50 μm channel length (L) and 1 mm width (W)). The real W/L value was measured (Figure 2F inset) to calculate the mobility values. The devices were characterized in a N_2 glove-box using a Keithley 4200-SCS semiconductor parameter analyzer. The measured capacitance of the BCB-covered SiO_2/Si substrates was 10 nF cm^{-2}, and was used for mobility calculation. For heat treatment, we heated the FETs based on the CH_2Cl_2-grown crystals under 100 ºC in N_2 glove-box for two hours and then cooled them down naturally.

Supporting Figures and Captions

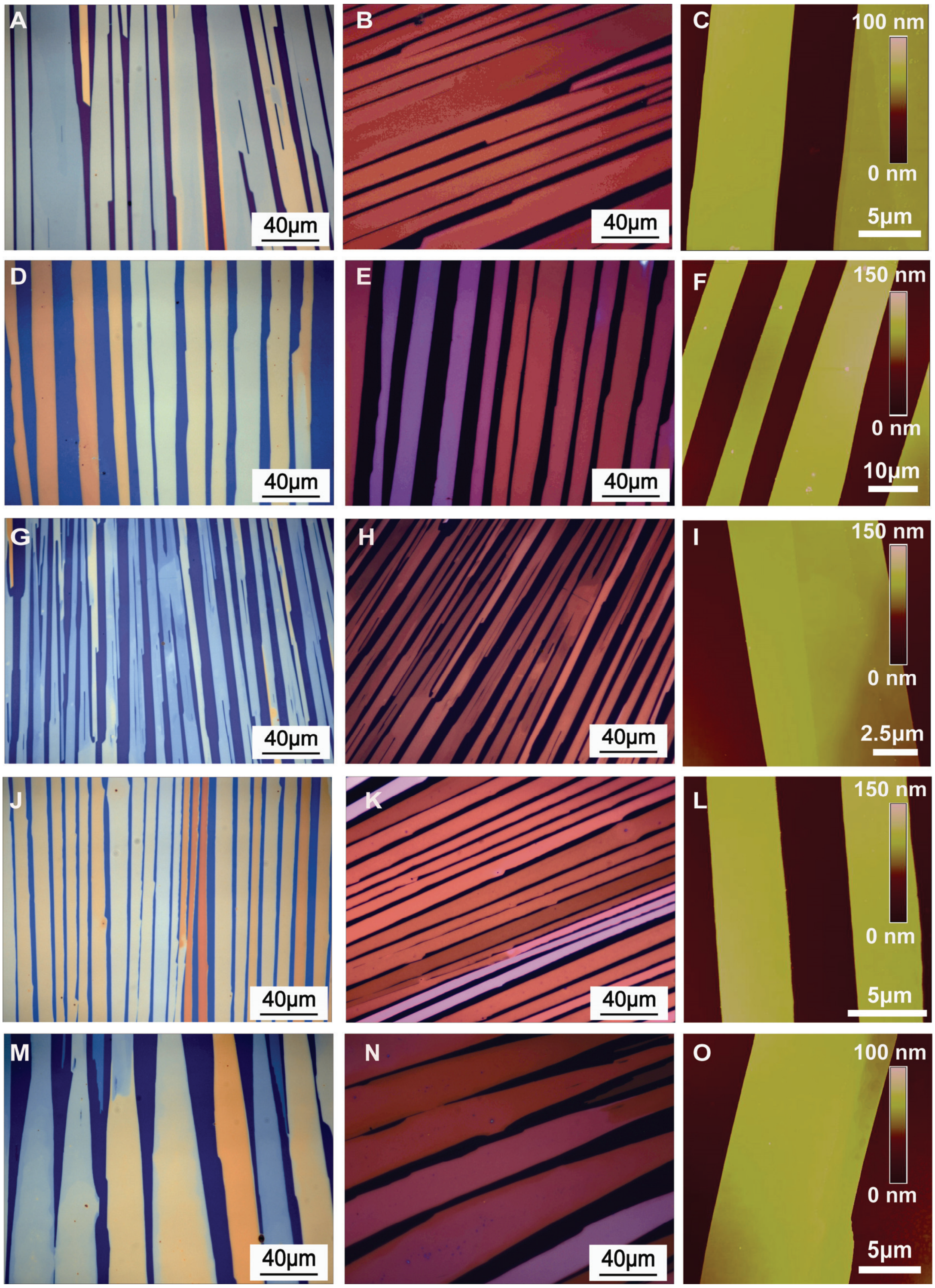

Fig. S1 Morphologies of well-aligned TIPS-pentacene crystals grown from (A-C) heptane, (D-F) cyclohexane, (G-I) $CHCl_3$, (J-L) CH_2Cl_2 and (M-O) THF, respectively. (A, D, G, J, M) OM images of the crystals, showing the alignment of the ribbons. (B, E, H, K, N) OM images of the crystals between crossed-polarizers. The images show uniform brightness throughout the crystals, indicative of single-crystallinity. (C, F I, L O) Atomic force microscopy (AFM) images of the crystals.

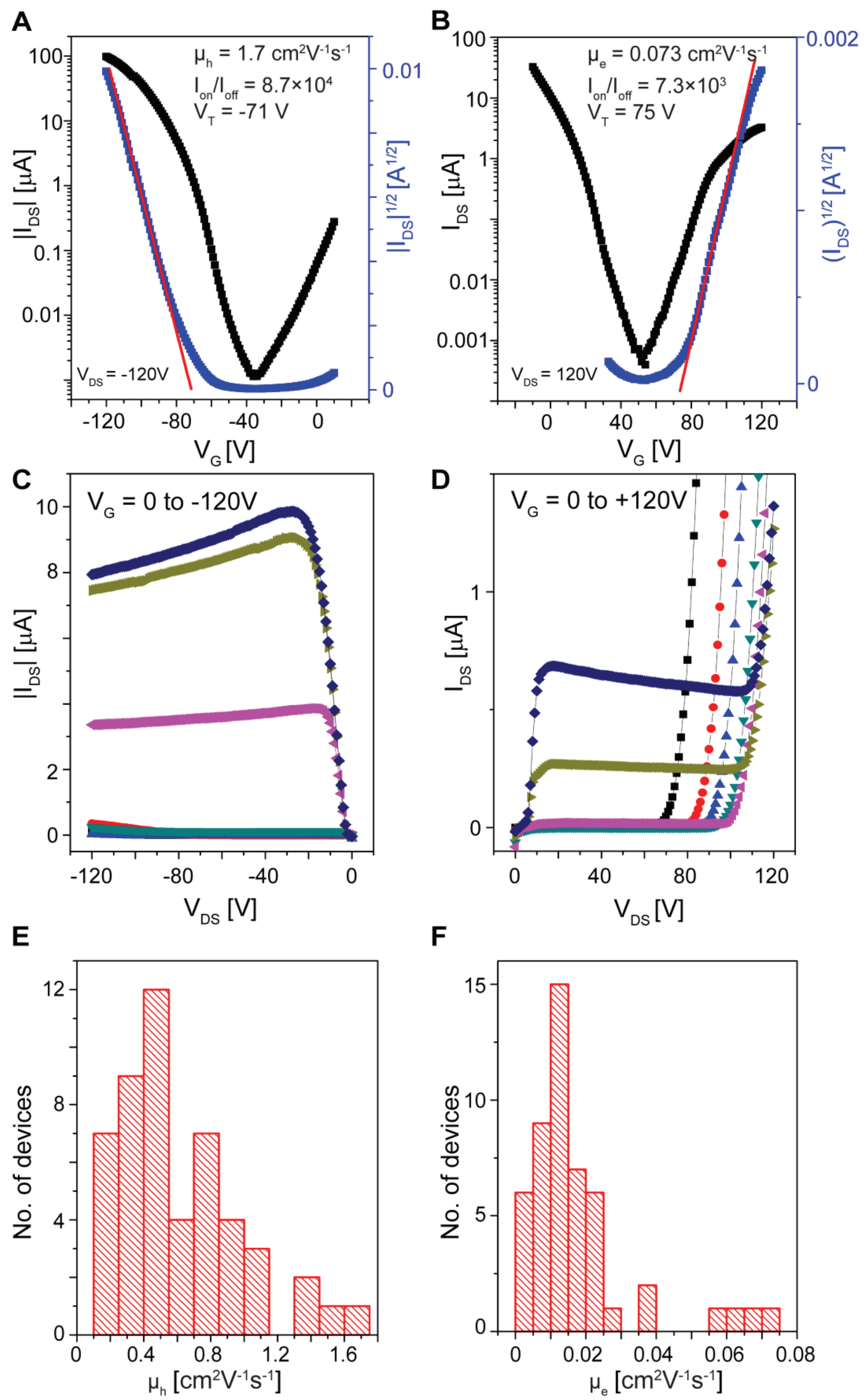

Fig. S2 FET characteristics of TIPS-pentacene single-crystals grown from heptane solutions. (A-D) Typical transfer and output characteristics of the FETs in p-channel operation mode (A, C) and n-channel operation mode (B, D). Device characteristics (μ, I_{on}/I_{off} and V_T) are shown in (A, B). (E) Histogram of the hole mobility of 50 FETs. μ_h of 0.62 ± 0.36 $cm^2V^{-1}s^{-1}$ (range: 0.19 to 1.7 $cm^2V^{-1}s^{-1}$), $I_{on}/I_{off}>10^3$, and V_T between -59 to -89 V were obtained. (F) Histogram of the electron mobility of 50 FETs. μ_e of $1.8\times10^{-2} \pm 1.6\times10^{-2}$ $cm^2V^{-1}s^{-1}$ (range: 4.0×10^{-4} to 7.3×10^{-2} $cm^2V^{-1}s^{-1}$), $I_{on}/I_{off}>10$, (48 out of 50, $>10^2$), and V_T between 64 to 90 V were obtained.

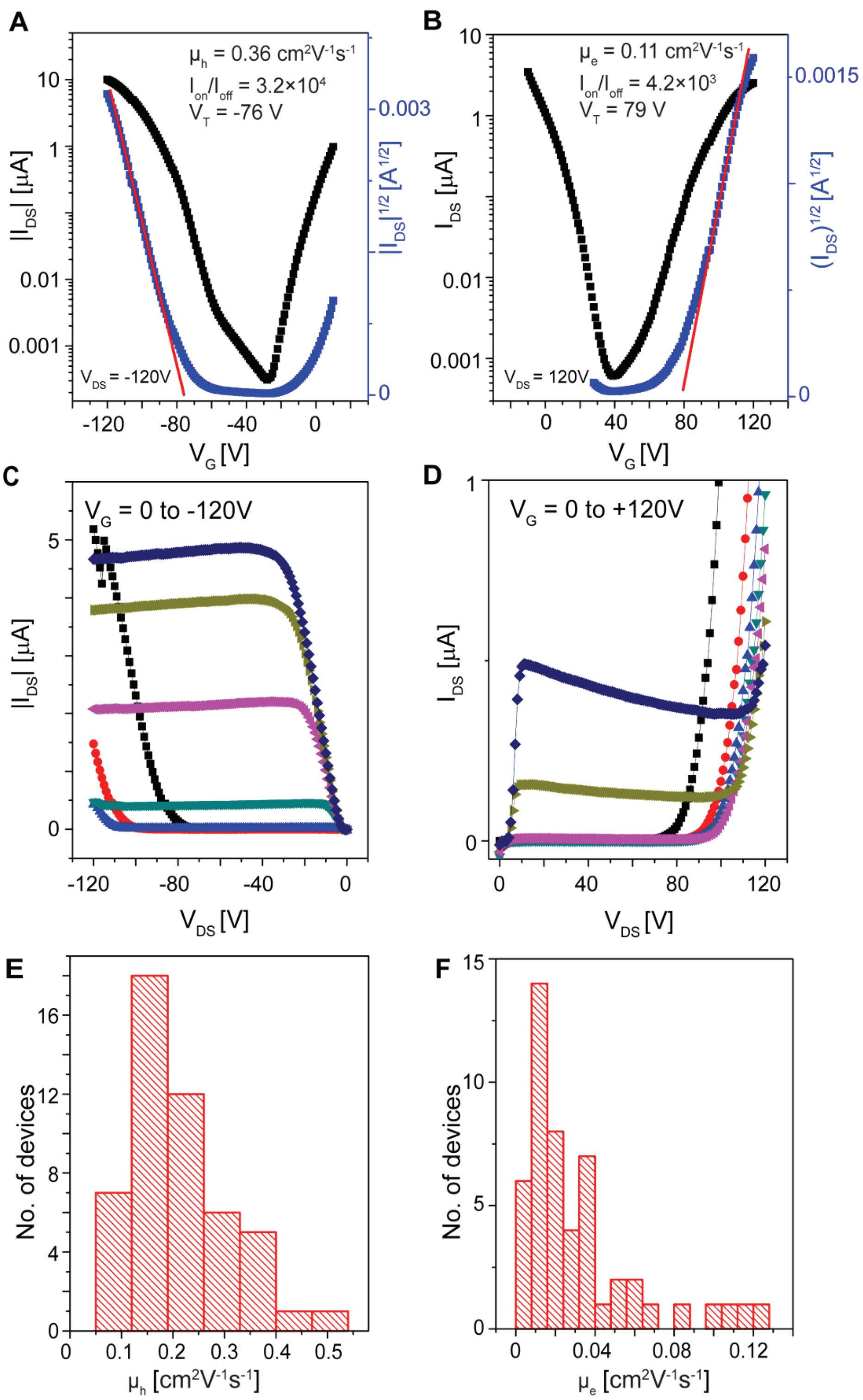

Fig. S3 FET characteristics of TIPS-pentacene single-crystals grown from cyclohexane solutions. (A-D) Typical transfer and output characteristics of the FETs in p-channel operation mode (A, C) and n-channel operation mode (B, D). Device characteristics (μ, I_{on}/I_{off} and V_T) are shown in (A, B). (E) Histogram of the hole mobility of 50 FETs. μ_h of 0.21 ± 0.090 $cm^2V^{-1}s^{-1}$ (range: 0.10 to 0.50 $cm^2V^{-1}s^{-1}$), $I_{on}/I_{off} > 10^3$, and V_T between -53 to -77 V were obtained. (F) Histogram of the electron mobility of 50 FETs. μ_e of $3.2\times10^{-2} \pm 2.9\times10^{-2}$ $cm^2V^{-1}s^{-1}$ (range: 3.3×10^{-3} to 1.3×10^{-1} $cm^2V^{-1}s^{-1}$), $I_{on}/I_{off} > 10$, (46 out of 50, $>10^2$), and V_T between 53 to 90 V were obtained.

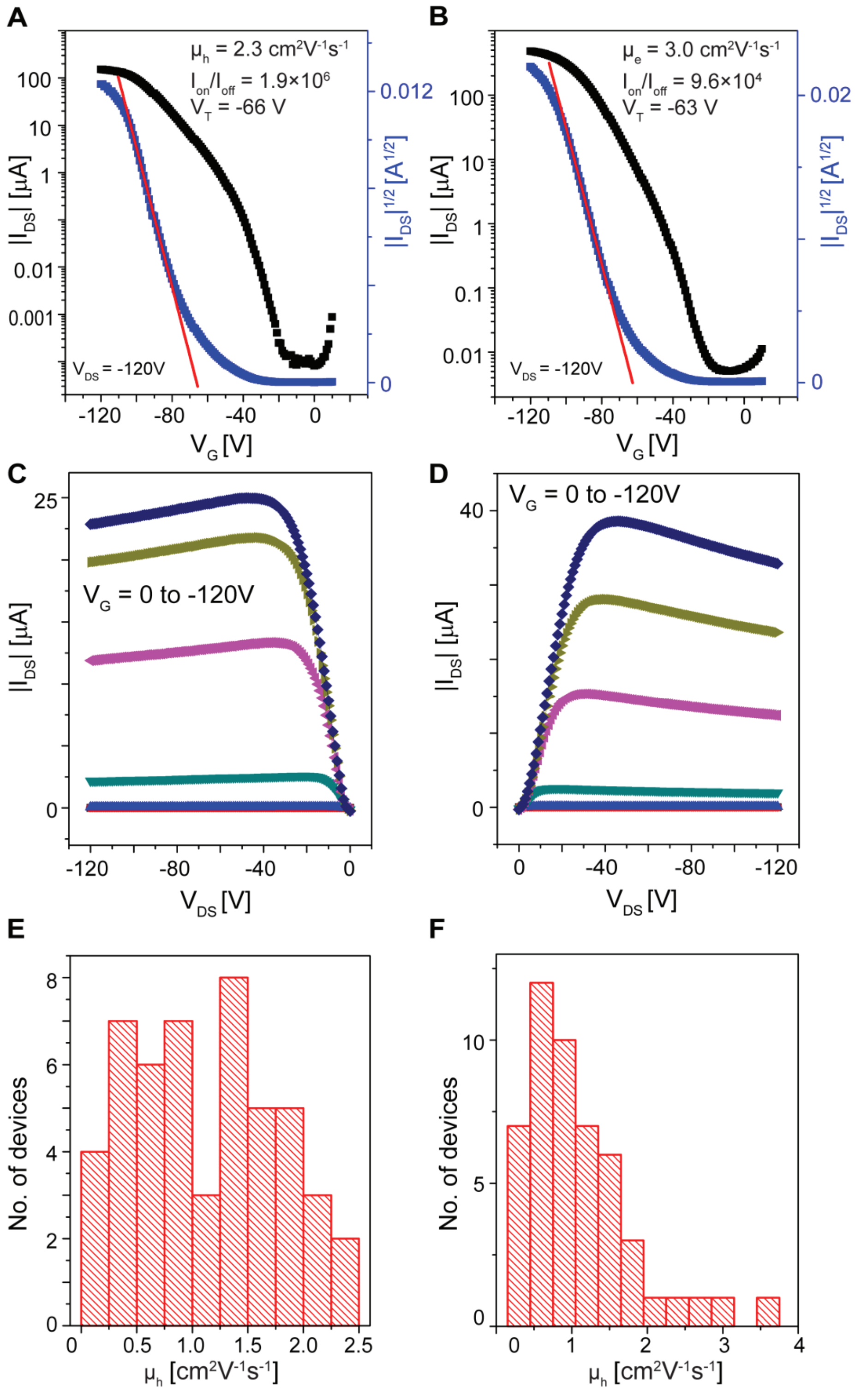

Fig. S4 FET characteristics of TIPS-pentacene single-crystals grown from THF (A, C, E) and $CHCl_3$ (B, D, F) solutions. (A-D) Typical transfer and output characteristics of the FETs in p-channel operation mode. Device characteristics (μ, I_{on}/I_{off} and V_T) are shown in (A, B). (E) Histogram of the hole mobility of 50 FETs based on crystals grown from THF solutions. μ_h of 1.13 ± 0.65 $cm^2V^{-1}s^{-1}$ (range: 0.12 to 2.3 $cm^2V^{-1}s^{-1}$), I_{on}/I_{off} >10^3, and V_T between -51 to -70 V were obtained. (F) Histogram of the hole mobility of 50 FETs based on crystals grown from $CHCl_3$ solutions. μ_h of 1.10 ± 0.73 $cm^2V^{-1}s^{-1}$ (range: 0.34 to 3.7 $cm^2V^{-1}s^{-1}$), I_{on}/I_{off} >10^4, and V_T between -30 to -78 V were obtained.

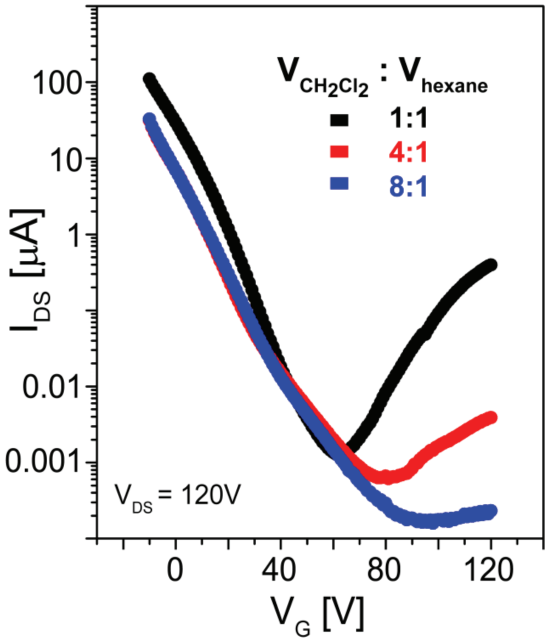

Fig. S5 Typical transfer characteristics of the FETs based on TIPS-pentacene grown from mixed solvents of CH_2Cl_2 and hexane in different volume ratios ($V_{CH_2Cl_2}$: V_{hexane} =1:1, 4:1, 8:1, respectively) in n-channel operation mode. The electron transport was found to be gradually suppressed as the concentration of CH_2Cl_2 increased. As the volume ratio reached 8:1, the devices exhibited no electron transport properties.

Reference

1 H. Y. Li, B. C. K. Tee, J. J. Cha, Y. Cui, J. W. Chung, S. Y. Lee and Z. N. Bao, *J. Am. Chem. Soc.*, 2012, **134**, 2760.

2 H. Y. Li, B. C. K. Tee, G. Giri, J. W. Chung, S. Y. Lee and Z. N. Bao, *Adv. Mater.*, 2012, **24**, 2588.

3 L. L. Chua, J. Zaumseil, J. F. Chang, E. C. W. Ou, P. K. H. Ho, H. Sirringhaus and R. H. Friend, *Nature*, 2005, **434**, 194.